EUROFUSION WPS2-PR(16) 14913

FM Castejon et al.

Neoclassical Transport And Iota Scaling In The Tj-Ii Stellarator

Preprint of Paper to be submitted for publication in
Fusion Science and Technology

This work has been carried out within the framework of the EUROfusion Consortium and has received funding from the Euratom research and training programme 2014-2018 under grant agreement No 633053. The views and opinions expressed herein do not necessarily reflect those of the European Commission.

NEOCLASSICAL TRANSPORT AND IOTA SCALING IN THE TJ-II STELLARATOR

F. Castejón[a], A. J. Rubio-Montero[b], A. López-Fraguas[a], E. Ascasíbar[a], and R. Mayo-García[b]

[a]Laboratorio Nacional de Fusión. CIEMAT. Av. Complutense 40. 28040, Madrid. Spain

[b]División de TIC. CIEMAT. Av. Complutense 40. 28040, Madrid. Spain

Abstract

Neoclassical transport properties are studied in TJ-II, taking effective ripple and plateau factor as the figures of merit. These two quantities have been estimated, using DKES code run by grid computing techniques, as functions of rotational transform and plasma volume. It was found that the effective helical ripple increases with plasma volume or rotational transform increase. This finding suggests degradation of confinement with iota or volume, which is in contradiction with the energy confinement scaling laws and with the TJ-II experimental results. The plateau factor is almost constant with the volume, but it rises following an almost quadratic law with the rotational transform, showing that the improvement of confinement with iota cannot be explained only by neoclassical transport in TJ-II.

I.-INTRODUCTION

Due to the complex nature of phenomena that define the plasma confinement in magnetic fusion devices, including transport and plasma-wall interaction, energy confinement time, τ_E, scaling laws are very useful tools to predict the properties of new devices and to check the validity of new theories. Experimental scalings show the parametric dependence of confinement on several plasma parameters, taking as basis the experimental results of a lot of plasma discharges of several machines of the same family but with different characteristics. Scaling laws are built based on the statistical properties of plasma confinement.

Scalings are used both in tokamaks and stellarators, but the strong differences between the two families of devices make that different scaling laws are built. In fact, it seems that turbulent transport dominates in the whole tokamak plasma (see e. g. Ref. 1), while neoclassical transport well explains the confinement of the stellarator core [2]. The toroidal symmetry and the existence of large plasma currents that contribute to create the magnetic field is the main difference between tokamaks and existing stellarators, which causes that the nature of transport be very different in both types of devices. Despite of this fact, both types of scalings show a positive dependence on the rotational transform, $\iota/2\pi$, the inverse of the safety factor, q. In tokamaks, Lackner-Gottardi scaling law[3] shows the following dependences for plasmas in the plateau regime with additional heating:

$$\tau_{Eplateau}^{LG} = C_p I_p^{4/5} \left(n_e / P\right)^{3/5} R^{9/5} a^{2/5} q^{2/5} \kappa / \left(1+\kappa\right)^{4/5} \qquad (1)$$

q is taken at ρ=2/3, being ρ the normalised minor radius. Where the constant $C_p \approx$ 1.2 10^{-13}, I_p is the plasma current in MA, n_e the line average electron density in m^{-3}, P the total injected power in MW, R the major radius in m, a the minor radius in m, and κ is the elongation. This scaling is written involving the parameters that fully define the tokamak configuration. The expression (1) can be written in terms of the rotational transform at the same position as:

$$\tau_{Eplateau}^{LG} = C_p \left(\iota / 2\pi\right)^{2/5} \left(n_e / P\right)^{3/5} R\ a^2 B^{4/5} \kappa \qquad (2)$$

A similar process produced the ISS95 scaling for stellarators, with a limited number of devices[4]:

$$\tau_E^{ISS95} = 0.079 a^{2.21} R^{0.65} P^{-0.59} n_e^{0.51} B^{0.83} \left(\iota_{2/3} / 2\pi\right)^{0.4} \qquad (3)$$

This expression includes discharges from ATF, CHS, Heliotron-E torsatrons, from W7-A shearless classical stellarator, and from W7-AS shearless optimised stellarator. In equation (3) all the quantities are in the same units of equations (1) and (2) but the density, which is written in 10^{19} m^{-3}. These latter units are also used in equations (4-8) of this paper. The first problem is that the stellarator configuration is much more complex than the tokamak one and cannot be defined by a few number of parameters. In fact, the authors of such scaling discussed the possibility of introducing a new parameter to distinguish the two latter stellarators

from the three former torsatrons. The rotational transform varies with radius so the convention of considering its value at normalised radius $\rho = 2/3$ is taken.

The more recent ISS04 scaling includes more stellarators all over the world with more discharges[5]:

$$\tau_E^{ISS04} = 0.134 a^{2.28} R^{0.64} P^{-0.61} n_e^{0.54} B^{0.84} \left(\iota/2\pi\right)^{0.41} \quad (4)$$

This equations is written in the same units as equation (3) and a positive dependence with respect to the rotational transform, taken again at $\rho = 2/3$, is observed. In such a work it was pointed out the necessity of establishing groups of devices with different devices that can be grouped by a factor f_{ren}, which accounts for the different confinement quality. In reference [6], the scaling is estimated including such a factor, finding:

$$\tau_E^{ISS04} / f_{enh} = 0.148 a^{2.33} R^{0.64} P^{-0.61} n_e^{0.55} B^{0.85} \left(\iota/2\pi\right)^{0.41} \quad (5)$$

This parameter depends on the configuration and can be related to the effective ripple as $f_{enh} \sim \varepsilon_{eff}^{0.4}$ in most of the stellarators (this scaling does not work properly in the quasi-helical symmetric HSX), showing that Neoclassical transport is an important ingredient in stellarator confinement.

Here, the factor f_{enh} represents the characteristics of the stellarator magnetic configuration that cannot be reflected by the scaling parameters. This factor is

introduced in order to make possible to fit all the confinement times of the devices to a single law. In any case, a positive dependence with the rotational transform is found again.

The rotational transform is a measurement of how twisted the magnetic field lines are. In fact, it is mandatory that the rotational transform is different from zero, in order that the confinement time reaches values of the order of ms or longer, since it is necessary to create magnetic surfaces and to avoid the ExB drift that would launch all the particles against the walls. Taking this fact into account, it is not striking that this positive dependence is found both in tokamaks and stellarators. We discuss here the relation between the rotational transform scaling and the neoclassical properties of TJ-II stellarator. The reminder of this paper is organised as follows. Section II is devoted to explain the properties of TJ-II confinement and its relation with the stellarator scaling laws. Section III discusses the neoclassical confinement properties of TJ-II, including their dependence on the rotational transform and volume and how this is related to the experimental confinement. The conclusions and discussion come in Section IV. We think that it is valuable to include an Appendix where the computational techniques used for this work are described, since they are not customary in the fusion community and involve some novelty themselves.

II.-TJ-II CONFINEMENT.

TJ-II is a four period flexible heliac[7], in operation since 1997. Its coil structure is composed of 32 toroidal field coils, four vertical field coils and a central conductor

made of two coils: a circular one and a helical one, which describes a four period helix around the circular coil (see figure 1). TJ-II flexibility comes from the fact that the properties of its magnetic configuration can be modified changing the currents that circulate in the coils. In particular, it is possible to substantially modify the plasma shape and volume, and the rotational transform of the configuration, allowing one to explore the influence of these quantities in the confinement.

After several years of experiments a large database of discharges under different magnetic configurations is available and has made possible to extract the confinement properties of TJ-II. The scaling for the energy confinement time of TJ-II in metallic wall is given by[8]:

$$\tau_E = 0.0131 a^{1.9} P^{-0.79} n_e^{0.68} \left(\iota_{2/3} / 2\pi\right)^{0.6} \quad (6)$$

while it is the following one for boronised wall:

$$\tau_E = 0.0295 a^{1.99} P^{-0.62} n_e^{1.01} \left(\iota_{2/3} / 2\pi\right)^{0.35} \quad (7)$$

The dependence on the major radius and the magnetic field has been suppressed in these expressions, since they cannot be varied in TJ-II. After a long period in which the TJ-II walls were covered with Boron, Li-coating techniques[9] were used to reduce the recycling, hence improving the density control and achieving larger values of the density in the device thus widening the operational regime, although

the dependence with rotational transform is under study yet. In fact, H mode confinement regime was achieved in TJ-II under these conditions[10].

These scaling laws show a positive dependence with the rotational transform as does the ISS04 scaling law. The dependence of confinement on the rotational transform extracted from equations (5) and (6) has two valuable properties. The first one is that TJ-II is an almost shearless device, hence the value of the rotational transform is almost the same in all the plasma and a single value can be assigned approximately to the global confinement. The second one is that the range of variation of this value in TJ-II flexibility diagram is the widest in the world, since it can vary from 0.9 to 2.5, so the dependence of energy confinement time on rotational transform can be explored experimentally in this device.

The approximately quadratic dependence of the confinement time with the minor radius in all the scalings seems easy to understand. The larger the volume the better the confinement, since the heat and the particles take longer to escape from the plasma. The volume is proportional to a^2, so this quadratic exponent shows just a linear dependence with the volume. Nevertheless, it is seen that the dependence with the volume is weaker than linear in TJ-II, which can be attributed to the properties of such a device. On the one hand, the confinement is improved for larger volume due to the effect of plasma size, on the other hand, the larger the volume, the larger the magnetic ripple, so the neoclassical transport of the outermost magnetic surfaces is worse, which mitigates the beneficial influence of the volume.

Scalings are basic to design new devices and to check the validity of new theories. It is necessary to work on the understanding of the dependence on the different parameters, including the rotational transform.

III.-SCALINGS AND NEOCLASSICAL CALCULATIONS

The parameters that appear in the ISS04 scaling law can influence the confinement properties in different ways, depending on the combination of parameters that are chosen, which is an effect of the fact that they are related among them. In fact, the ISS95 scaling law presented similar dependencies, as can be seen in equation (3), despite of the fact that it is based on the results of fewer devices than the ISS04 scaling law, which includes TJ-II, for instance. The dependence with *R* and *a* changes in this scaling law if one suppresses the rotational transform dependence, i. e., when less parameters of the configuration are included in the scaling:

$$\tau_E^{ISS95} = 0.0132 a^{1.51} R^{1.04} P^{-0.62} n_e^{0.53} B^{0.81} \qquad (8)$$

The regression analysis has RMSE (Root Mean Square Error) equal to 0.0902 when iota is considered in comparison with 0.0909, when it is not. This increase, although small, is statistically significant. The change is due to the fact that the ISS95 scaling law was built with the results of an optimised advanced stellarator (W7-AS) and three torsatrons (ATF, H-E, CHS), and in these latter devices iota is related to the ratio R/a, the aspect ratio.

No explanation has been given up to now for the positive scaling of the confinement time with the rotational transform. Hinton and Hazeltine[11], and more recently Belli and Candy[12], obtained the neoclassical transport coefficients semi-analytically for a large aspect ratio tokamak, showing an explicit dependence on the rotational transform, which drives one to believe that this parameter has influence on the neoclassical properties of the device. For a given effective collisionality, the neoclassical transport coefficients vary with iota as $D_{NC} \propto q^2 = \left(\iota / 2\pi\right)^{-2}$, in the banana regime, showing the same tendency as the scaling laws that predict an improvement of the confinement with the inverse of *q*. In the plateau regime, $D_{NC} \propto \iota^{-1}$, yielding the result $\tau_E \propto \iota^{0.4}$. So the variation with iota of the neoclassical confinement in a tokamak is in agreement with the one of scaling laws. In a tokamak, neoclassical transport and turbulent one diminish with the rotational transform.

The main configuration ingredient that originates neoclassical transport is the magnetic ripple. In an axisymmetric tokamak, the magnetic ripple along a field line appears because of the variation of the magnetic field as the poloidal angle is evolved, therefore it is related to the rotational transform. In a stellarator no such a clear dependence can be extracted, since there is more freedom to design the magnetic configuration. In order to check the possible relation between the iota scaling and the neoclassical transport in stellarators, we estimate significant geometrical quantities, which describe the properties of the configurations, namely the effective ripple, defined in Eq. (9) and the plateau factor, defined in Eq. (10). These quantities have been estimated performing extensive neoclassical transport calculations have been performed in TJ-II by the use of the DKES code[13]. These

calculations have been performed using advanced grid computing techniques that are described in the Appendix.

III.A- The effective ripple.

The neoclassical transport properties of a configuration in the long mean free path are summarised in a single parameter, the effective ripple, ε_{eff} ,given by[14]:

$$\varepsilon_{eff} = \lim_{\nu^* \to 0} \left[2 \left(\left(\frac{3\pi}{4} \right)^{1/2} \nu^* D_{11}^* \right)^{2/3} \right] \qquad (9)$$

Where $\nu*$ is the effective collsionality ($\nu^*=\nu qR/\mathrm{v}$) and D_{11}^* is the first mono-energetic coefficient of neoclassical transport matrix. The effective ripple gives a clear idea of the quality of the magnetic configuration for the neoclassical confinement, without the necessity of exploring different collisional regimes. The effective ripple can be estimated in a quicker way using a formula introduced in Ref. 15 in the $1/\nu$ regime. Nevertheless, we have used the method of equation (9) because we have already ported the DKES code to the grid and can take advantage of such a computing platform.

Given the flexibility of TJ-II, independent scans of rotational transform and volume can be performed. The magnetic ripple rises with the volume since the plasma is closer to the coils in the larger configurations, being more sensitive to the variation of the magnetic field. So it is possible to explore the effect of both quantities on the effective ripple.

We have taken 5 different volumes, with similar values of the rotational transform, and 6 different values of the rotational transform for approximately constant volume. In this way, we have considered 30 configurations that scan volume and rotational transform. Figure 2 shows these 30 configurations located in the so called flexibility diagram, showing the different rotational transform and the volume values. Figure 3 shows the magnetic surfaces at toroidal angle ϕ=0 for 4 extreme configurations plus the central one: minimum iota and minimum volume, minimum iota and maximum volume, maximum iota and minimum volume, maximum iota and maximum volume and intermediate values of iota and volume. It can be seen that the distance of the plasma to the toroidal coil is smaller for the larger volume, therefore those configurations present larger magnetic field ripple. So one can expect that these configurations present worse neoclassical transport properties.

The large iota configurations present indented magnetic surfaces, which makes the plasma-wall interaction (PWI) to be weaker in these cases, since the zone of the groove of the TJ-II vacuum vessel presents the strongest PWI in the device [16], so elongated configurations will have less influence of PWI. This dependence of plasma-wall interaction and the rotational transform can explain the different scaling laws with the rotational transform found in TJ-II for the different first wall material, being stronger in the cases of metallic wall where the plasma-wall interaction has stronger influence on confinement.

The effective ripple given by equation (9) is calculated for every radial position of these configurations. In fact we take 23 radial points for every configuration, therefore with slightly different values of iota. The effective ripple is shown in Figure 4 for all the configurations and radii, as a function of volume and iota. As the rotational transform is not constant along the minor radius, a curve of ε_{eff} is shown as a function of iota for a given magnetic configuration. We see that iota is negative in TJ-II, because of choice of the magnetic coordinate system, but the absolute value of iota must be taken in the above shown scaling laws.

In order to explore the variation of ε_{eff} at different radial positions and, hence, how the neoclassical transport depends on those two parameters in the long mean free path, we plot the effective ripple at three positions: ρ=0, 0.65, 1. Figures 5a and 5b show the variation of ε_{eff} as a function of the rotational transform and the volume at the position ρ=0, showing that the effective ripple increases slightly with the volume at this radial position, which is not surprising, given the characteristics of the TJ-II stellarator and the larger excursion of the magnetic axis for larger magnetic configurations. The dependence with the rotational transform is not monotonic and depends on the configuration that is considered, although an increasing trend with increasing absolute value of iota can be seen.

Figures 6a and 6b show the same as figures 5a and 5b for ρ = 0.65 ≈ 2/3, located in the pressure gradient zone of the plasma, hence having more influence on transport. Again, an increase of the effective ripple with the volume is shown, as can be understood following the discussion above about Figure 3, and a less pronounced non-monotonic behaviour with iota appears. In fact, the effective

ripple almost rises with the rotational transform, which should provide a dependence with rotational transform opposite to the one observed in the scaling laws and in the semianalytical calculations for tokamaks.

Finally, ε_{eff} is plotted as a function of iota and the volume in Figures 7a and 7b for ρ=1, with the same tendency with volume and a non-monotonic variation with iota for the larger volumes and an increasing ripple for small volumes, showing again a behaviour opposite to what it is expected form the scaling laws and the semianalytical estimates for tokamaks.

As it has been pointed above, the parameter that appears in the ISS04 scaling, f_{enh}, can be related with the effective ripple as $f_{enh} \sim \varepsilon_{eff}^{0.4}$, showing that effective ripple is an important ingredient in stellarator confinement, although this scaling does not work properly for HSX.

LHD team has shown that, in this device, the neoclassical confinement properties can be improved by changing the position of magnetic axis and, hence, the value of major radius: DKES calculations show that the lower the radius the better the neoclassical confinement properties [17]. Moreover, gyrokinetic calculations show that improving the neoclassical confinement goes in the same direction as doing it with the turbulent transport[18]. According to this result, optimizing a device from the neoclassical point of view would be also beneficial for reducing turbulent transport. Experiments in HSX show that the quasisymmetric configuration presents lower viscosity than the mirror one[19], together with better confinement properties. So the neoclassical viscosity plays also a role on confinement. In fact,

recent results in TJ-II show that it is possible to reduce the neoclassical viscosity in the point where the electric field passes from electron to ion root, which decreases strongly the flow damping[20]. Nevertheless, scaling law of Eq. 9 has shown that iota value is linked to the aspect ratio in torsatrons, which is also related to magnetic ripple. So the link between neoclassical and turbulent optimization cannot be extended to all the stellarator configurations.

The dependence of the confinement with the rotational transform cannot be explained in terms of the neoclassical properties of the device, as calculations for TJ-II show. On the opposite, a global increase of the effective ripple with iota could be extracted for small volumes in TJ-II discharges that goes against the scaling laws that have been obtained up to know.

III.B- The plateau factor.

The effective helical ripple provides a measure on the quality of Neocñassical confinement in the long mean free path regime, i. e., where the trasnport coefficient depend on the collsionality as $1/\nu$. This is because the effective ripple quantifies how strongly drift surfaces differ from flux surfaces, so the above considerations are valid in the lmfp regime. Nevertheless, the so called plateau factor plays the same role in the collisional plateau regime[21] and it is also a geometrical factor that can be studied from the configuration equilibrium. The normalised plateau factor is given in Boozer coordinates as:

$$\Gamma_{norm} = |\iota/2\pi| \sum_{m,n} \left(\frac{m b_{m,n}}{\varepsilon_t} \right)^2 \frac{1}{|m\iota/2\pi - nN|}$$

(10)

Where N is the period number, ε_t = r/R is the inverse aspect ratio of the surface with effective radius r=a ρ , and $b_{m,n}$ are the values of the Fourier harmonics with poloidal and toroidal mode numbers n amn m, respectively. This factor is normalised in such a way that the simplest tokamak with circular surfaces and magnetic field given by B/B0 = 1 + $b_{1,0}$ cos θ will have Γ_{norm} = 1.

We estimate now the plateau factor of Eq. 10 for all the TJ-II configurations considered in this paper by performing the summation in Equation (10) over all $b_{m,n}$ in the TJ-II magnetic field spectrum in Boozer coordinates.

Now we can follow the approach of Dinklage et al.[22] one can write the absoebed power in steady state as:

$$P \approx n_e T \left(\frac{\Gamma_{norm} T^{3/2}}{B^2} \frac{2\pi}{\iota} \right) \tag{11}$$

We can extract the electron temperature and introduce it in the energy confinement expression. One will have:

$$\tau_E \propto \frac{nT_e}{P} P \propto \left(n_e/P\right)^{3/5} B^{4/5} \left(\left(\iota/2\pi\right) / \Gamma_{norm} \right)^{2/5} \tag{12}$$

This expression shows a dependence of the energy confinement time with respect to the rotational transform very similar to the above shown scaling laws ISS95 and ISS04: $\iota^{0.4}$, but the confinement time is now written as a function of the plateau

factor, which is a function of the magnetic configuration. If this factor is the same for all the configurations, this means that the TJ-II scañling is governed by the neoclassical transport in the ion plateau regime.

We represent Γ_{norm} for all the considered configuration as a function of the volume and the rotational transform in order to check if the dependence found in the scaling laws can be attributed to this quantity.

Figures 8a and 8b show Γ_{norm} as a function of the volume, for the radial positions $\rho \approx 0.65$ and 1, respectively, for the different values of the rotational transform. It is seen that the plateau factor depends weakly on the magnetic configuration. Figures 9a, 9b show Γ_{norm} as a function of the rotational transform, for the radial positions $\rho \approx 0.65$ and 1, respectively, and for the different values of the volume.

It is seen in figures 9a and 9b that the plateau factor rises with the rotational transform following a quadratic law $\Gamma_{\mathrm{norm}} \sim \iota^2$, with the exception of the highest rotational transform values, which show a different behaviour, meaning that the scalings cannot be explained by the variation of plateau factor with the configuration.

All these facts mean that the neoclassical optimization helps to the reduction of turbulent transport, but it is not the only ingredient to be considered in the turbulent optimization of the stellarators. The positive rotational transform dependence of confinement must be attributed to a turbulent mechanism and open new doors to stellarator optimization.

IV.-CONCLUSIONS AND DISCUSSION

We have shown that the neoclassical confinement of TJ-II in the long mean free path regime is not improved for higher values of the rotational transform. In fact, TJ-II characteristics show that the neoclassical transport properties in the $1/\nu$ regime, given by the effective ripple, are improved with the volume and not with the rotational transform. This latter parameter is coupled to the poloidal ripple in an axisymmetric tokamak, hence showing influence on the neoclassical transport, while it is decoupled in a stellarator, since the magnetic configuration is created by external coils and not by the plasma current. Nevertheless, torsatrons present also some relation between the aspect ratio and the rotational transform, which implies some relation between neoclassical optimization and increasing iota.

The neoclassical confinement properties of the device in the ion plateau regime are given by the configuration dependent plateau-factor. It is seen in TJ-II a clear dependence of the plateau factor on the rotational transform, which should not be the case to explain the iotas-dependence of ISS04 and ISS95 scaling laws in temrs only of neoclassical transport.

Therefore, the explanation for the improvement of confinement with the rotational transform cannot be given by neoclassical transport either in the $1/\nu$ or in the ion plateau regime. It is necessary to explore the turbulence properties of the configuration in relation with such a parameter. This assessment implies that the reduction of turbulent transport in a stellarator cannot be performed only by optimising the neoclassical transport, since there are other phenomena that must be considered.

Electrostatic turbulence could play a role as well as MHD. For instance, Global Acoustic Modes, which are able to regulate turbulence[23], in a similar way in which

Zonal Flows do, are shown to suffer more damping for large values of q, or, equivalently, for small values of the rotational transform. In a tokamak, the growth rate is given by $\gamma_{GAM} \alpha [- exp(-cq^2)]$ (See referene 24). We do not expect that this simple formula is working for stellarators, but it has been shown that the damping of the GAMs behaves in TJ-II in the same way of tokamaks: it rises with q, as can be seen in Reference 25. More experimental and theoretical work is needed to clarify the reasons for the positive influence of iota on the confinement.

APPENDIX

Grid computing emerged as a powerful infrastructure for executing distributed applications. Mainly developed to give computing support to the four Large Hadron Collider (LHC) experiments, it was adopted by other scientific disciplines such as Biomedicine, Bioinformatics, Earth Sciences or Fusion. In the latter case, grid computing techniques were incorporated to fusion research for calculations that can be performed in a distributed way[26]. Examples of the successful use of Grid Computing for fusion are the porting codes devoted to the simulation of different phenomena such as Neutral Beam Injection[27], ion orbits inside the plasma[28], optimization of stellarators[29], or core turbulence simulations[30]. Grid is also used coupled to a parallel supercomputer, creating a heterogeneous workflow to estimate electron Bernstein wave heating in TJ-II (see reference 31). Grid computing has been also used to calculate large datasets that can be introduced in a database, as the case of the estimation of the monoenergetic neoclassical coefficients using the grid version of DKES, which is used for the present work[32].

Nevertheless, grid infrastructures have some caveats, as the missing of jobs, that affect the computational efficiency, so several methodologies have been developed in the latest years to improve it. Among them, we have developed a method based on the use of pilot jobs, i.e. a master-slave approach within a grid environment that reduces the waiting time in remote queues by means of remote a slot appropriation. Thus, when a pilot job starts running on a node, it allows the workload management system to directly use and monitor that node.

Moreover, the interest in monitoring the pilots is not only related to effectively characterise the assigned resources (the Working Nodes) by simply notifying the existent configuration and properties to the master. Monitoring is indispensable to check and prepare the environment (downloading and installing software) needed by many scientific applications. Therefore, this mechanism enables compatibility with legacy systems.

Fusion community has successfully tested several pilot systems to improve its scientific throughput. In this sense, ISDEP has been adapted to Ganga and DIANE[33], and tested on DIRAC test-bed, but this approach has not actually come into production because of adaptability and maintenance issues. Additionally, specific implementations similar to pilot-jobs have been done to adapt the DAB stellarator optimization code[34].

Recently, a new pilot-job approach[35] has been implemented to complement the meta-scheduler GridWay ecosystem[36]. GWpilot provides an automatic and unattended use of pilot jobs by both users and developers. It maintains all the

GridWay features but adding new ones that can be useful for any multidisciplinary community. Therefore, this framework can directly support the execution of the aforementioned fusion applications, ant it also enables the straightforward adaptation of any legacy one coming from other scientific areas. GWpilot has been used to run DKEsG, which has been used to obtain the effective ripple given by Eq. (9) of this work.

Acknowledgements

The authors would like to thank Dr. J. L. Velasco for his support running DKES code. This work has been carried out within the framework of the EUROfusion Consortium and has received funding from the Euratom research and training programme 2014-2018 under grant agreement No 633053. The views and opinions expressed herein do not necessarily reflect those of the European Commission. This work has been carried out also with the support of the Spanish Ministry of Economy and Competitiveness funded projects CODEC (TIN2013-46009-P) and ENE2014-52174-P.

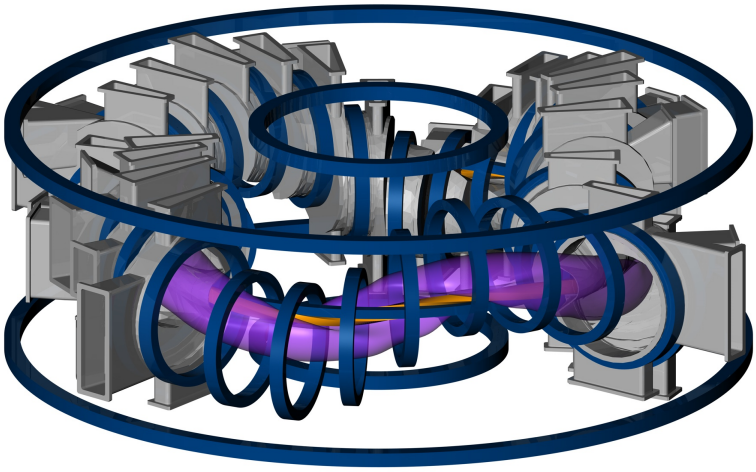

Figure 1

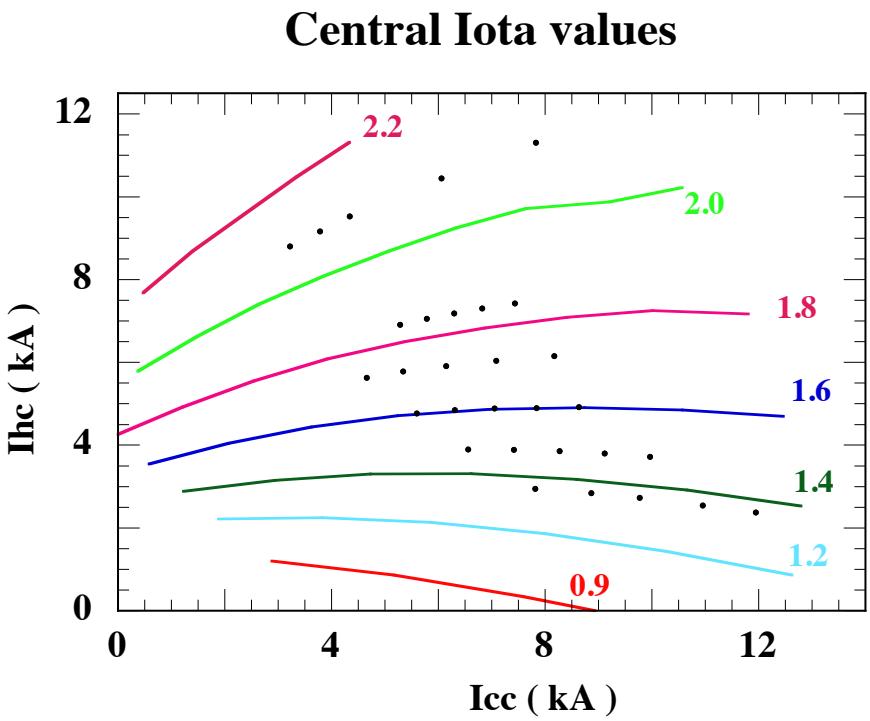
Central Iota values
12
8
4
0
Ihc (kA)
0
4
8
12
Icc (kA)
2.2
2.0
1.8
1.6
1.4
1.2
0.9

Figure 2.

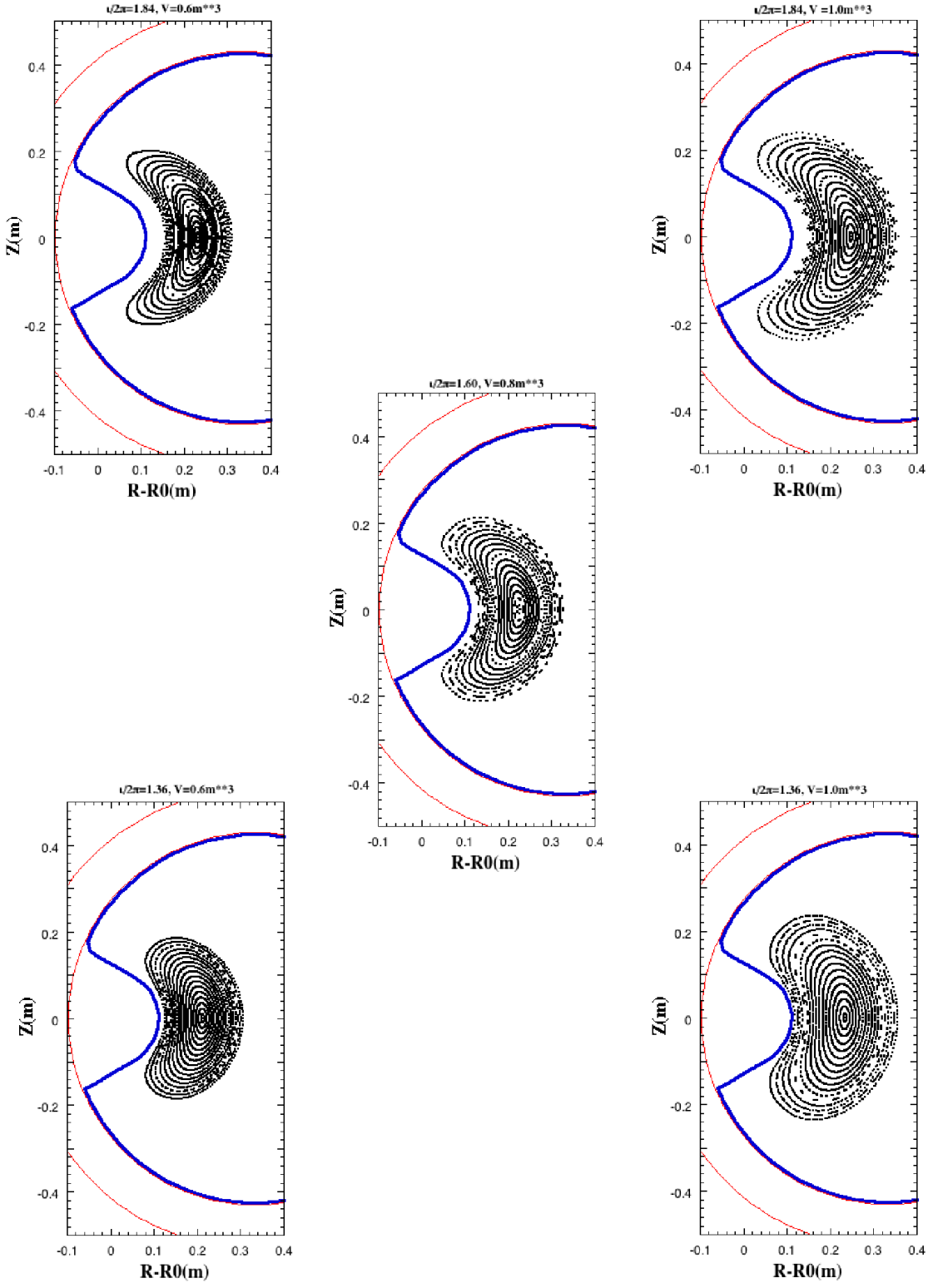
ι/2π=1.84, V=0.6m**3
ι/2π=1.84, V =1.0m**3
ι/2π=1.60, V=0.8m**3
ι/2π=1.36, V=0.6m**3
ι/2π=1.36, V=1.0m**3
Z(m)
R-R0(m)

Figure 3.

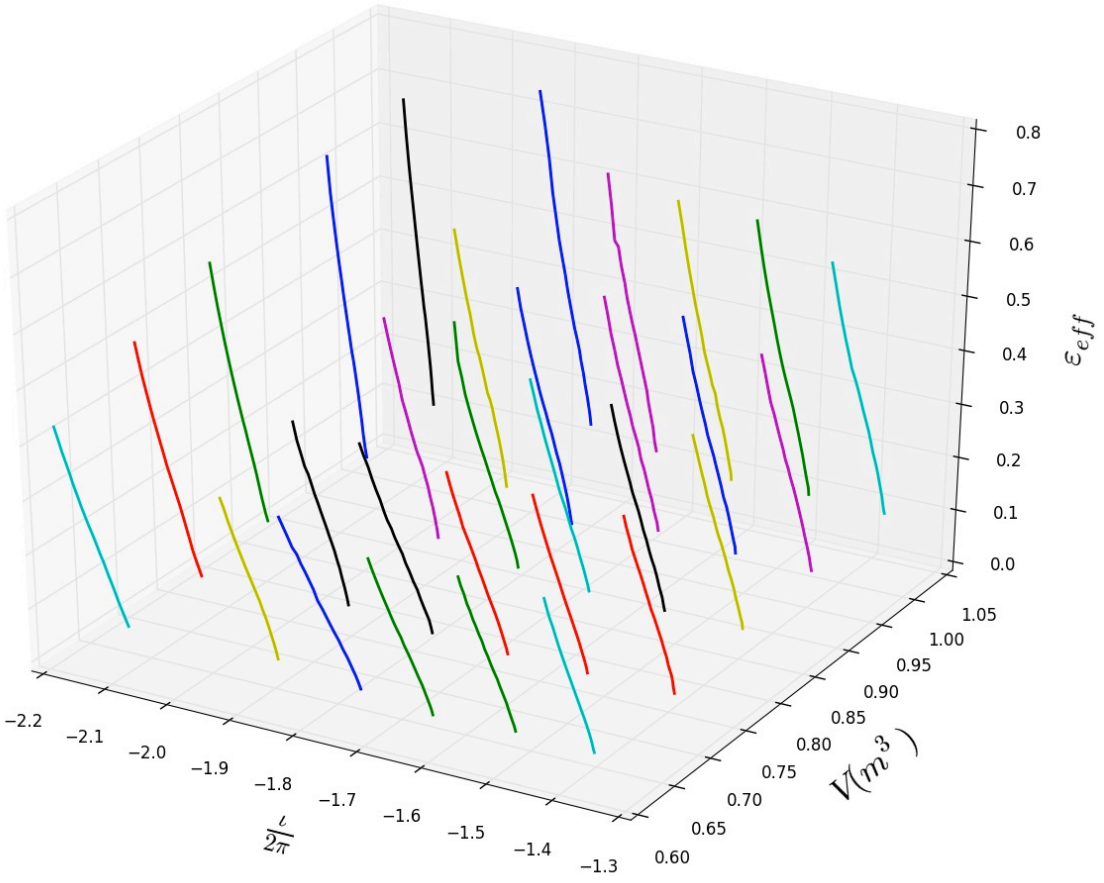
0.8
0.7
0.6
0.5
0.4
0.3
0.2
0.1
0.0
ε_{eff}
1.05
1.00
0.95
0.90
0.85
0.80
0.75
0.70
0.65
0.60
$V(m^3)$
−2.2
−2.1
−2.0
−1.9
−1.8
−1.7
−1.6
−1.5
−1.4
−1.3
$\frac{\iota}{2\pi}$

Figure 4.

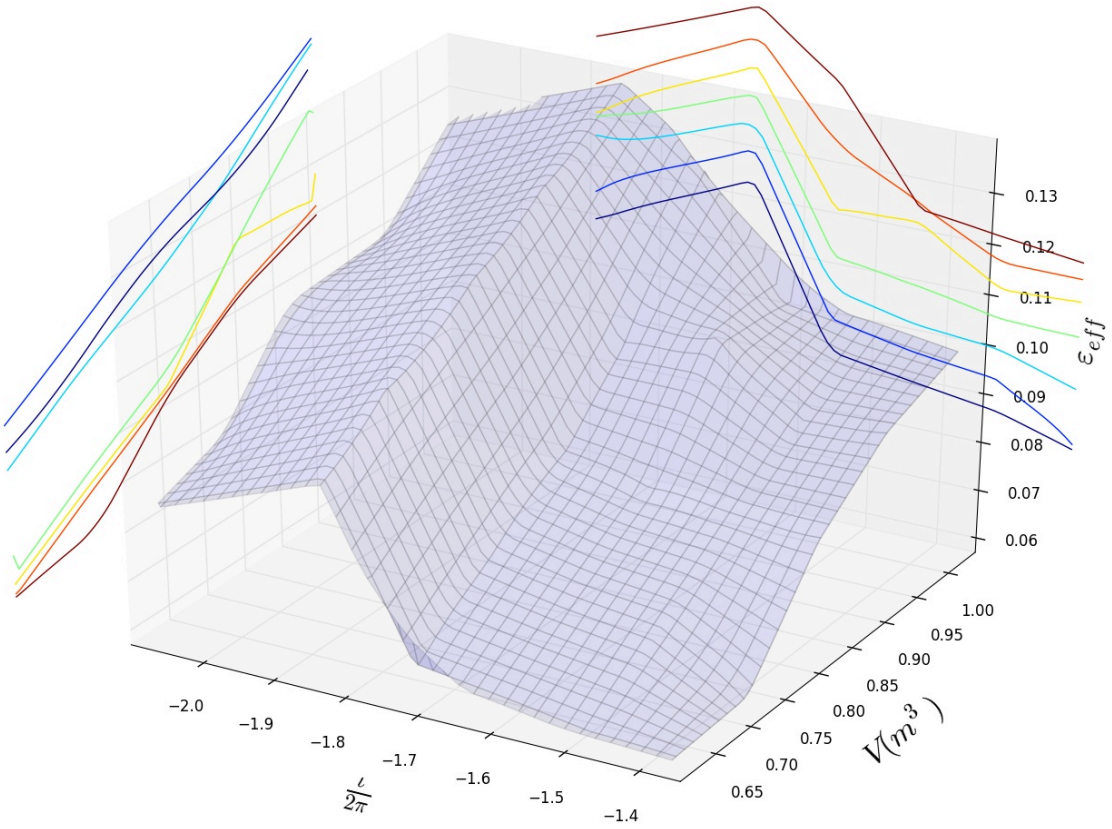
0.13
0.12
0.11
0.10
0.09
0.08
0.07
0.06
ε_{eff}
1.00
0.95
0.90
0.85
0.80
0.75
0.70
0.65
$V(m^3)$
−2.0
−1.9
−1.8
−1.7
−1.6
−1.5
−1.4
$\frac{\ell}{2\pi}$

Figure 5a.

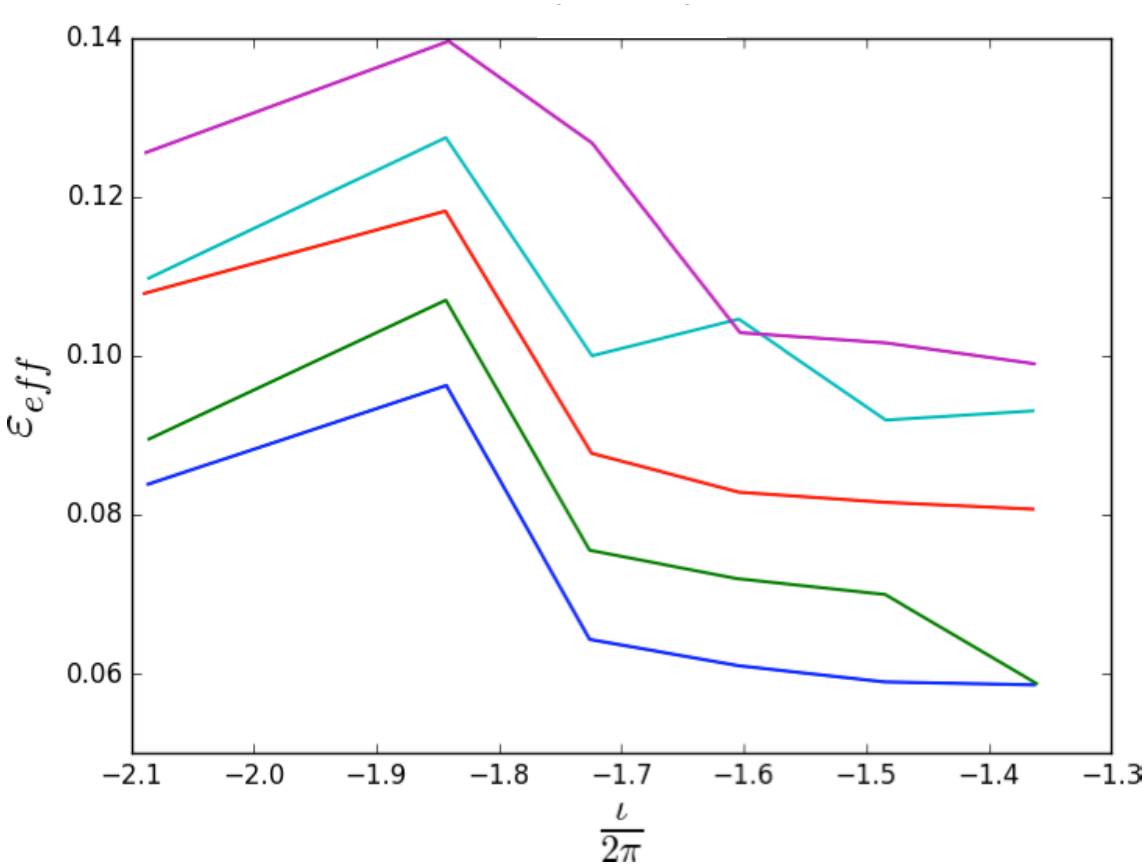
0.14
0.12
0.10
0.08
0.06
ε_{eff}
−2.1
−2.0
−1.9
−1.8
−1.7
−1.6
−1.5
−1.4
−1.3
$\frac{\iota}{2\pi}$

Figure 5b.

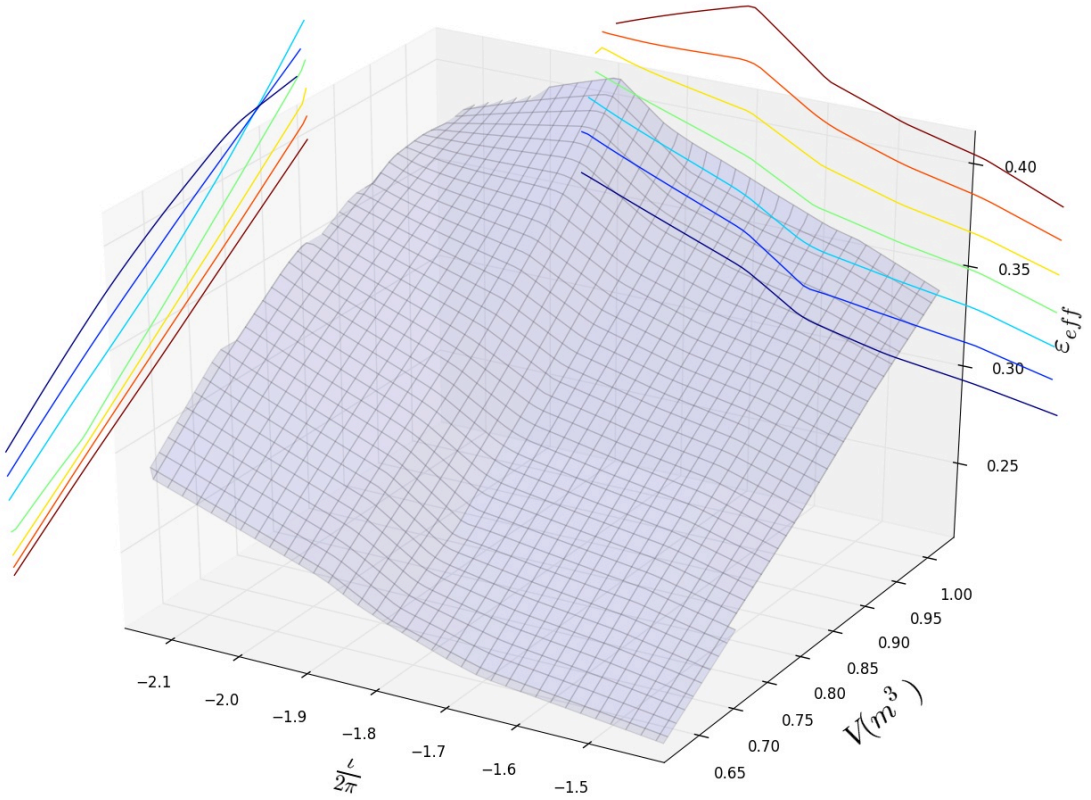

Figure 6a: The same as figure 5a for ρ=0.65.

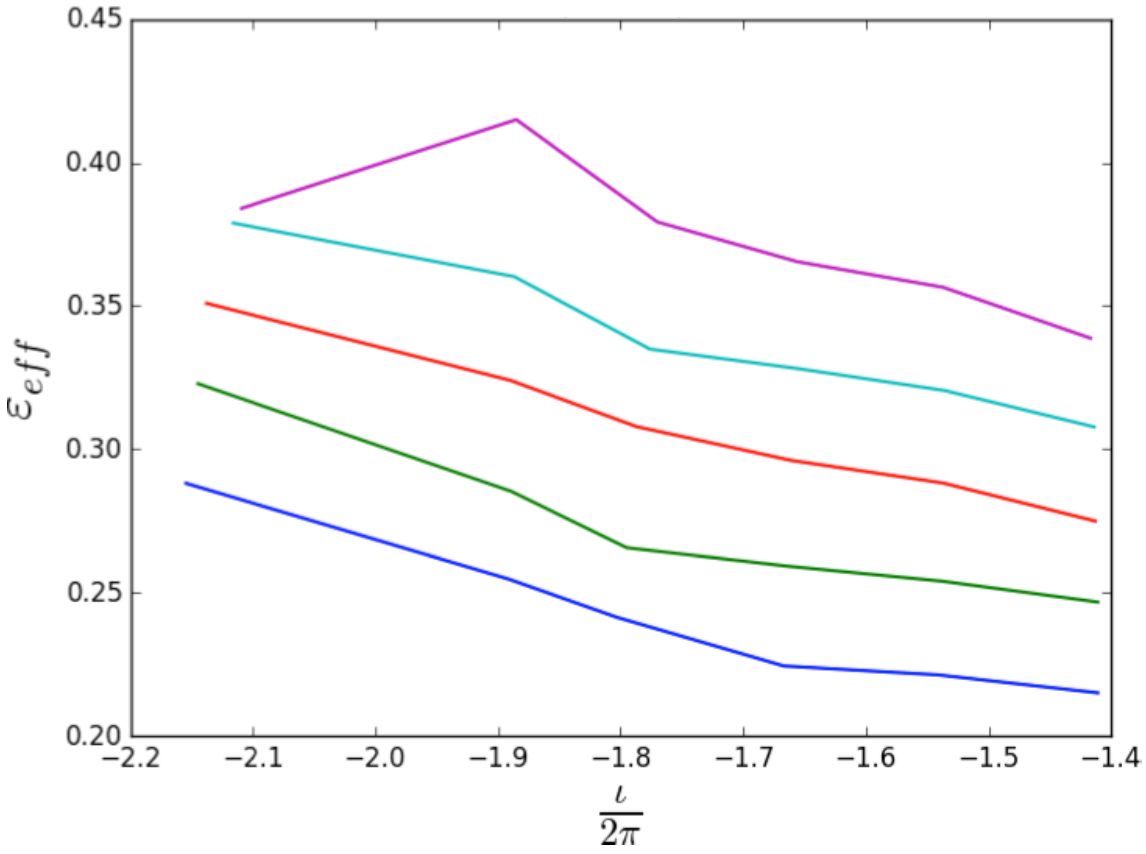
0.45
0.40
0.35
0.30
0.25
0.20
ε_{eff}
−2.2
−2.1
−2.0
−1.9
−1.8
−1.7
−1.6
−1.5
−1.4
$\frac{\iota}{2\pi}$

Figure 6b.

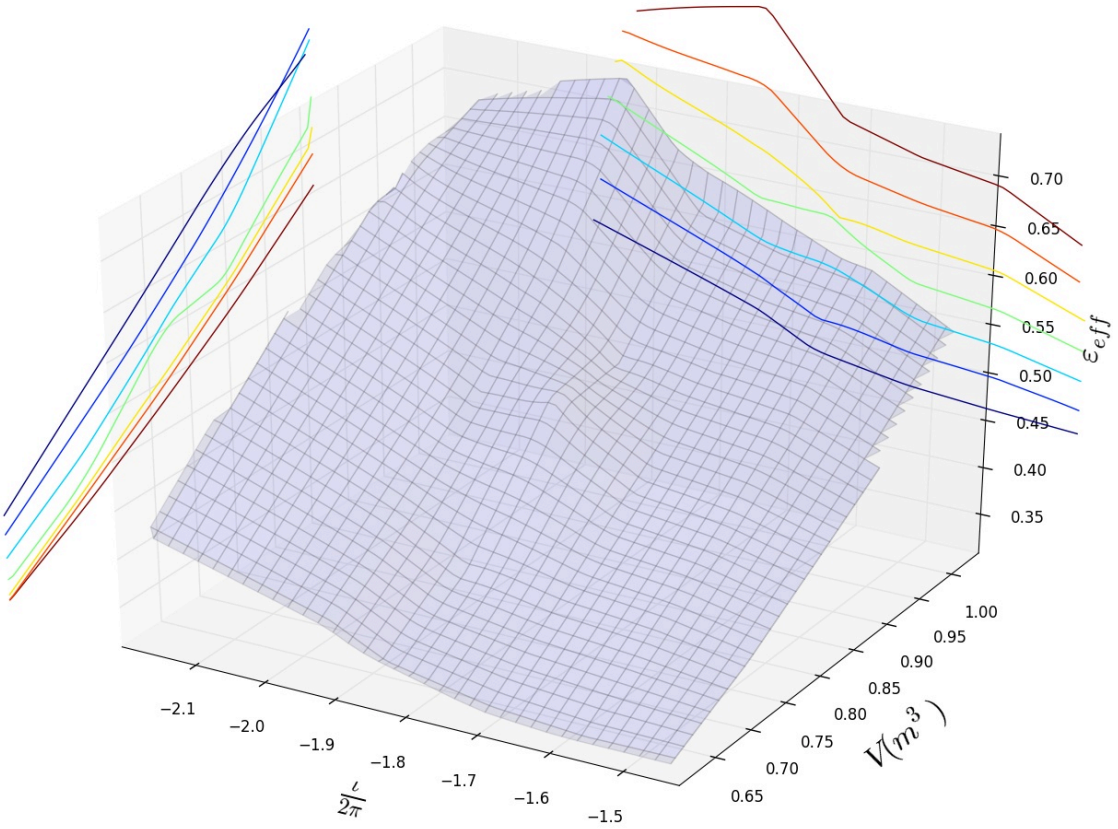
0.70
0.65
0.60
0.55
0.50
0.45
0.40
0.35
ε_{eff}
1.00
0.95
0.90
0.85
0.80
0.75
0.70
0.65
$V(m^3)$
−2.1
−2.0
−1.9
−1.8
−1.7
−1.6
−1.5
$\frac{\gamma}{2\pi}$

Figure 7a.

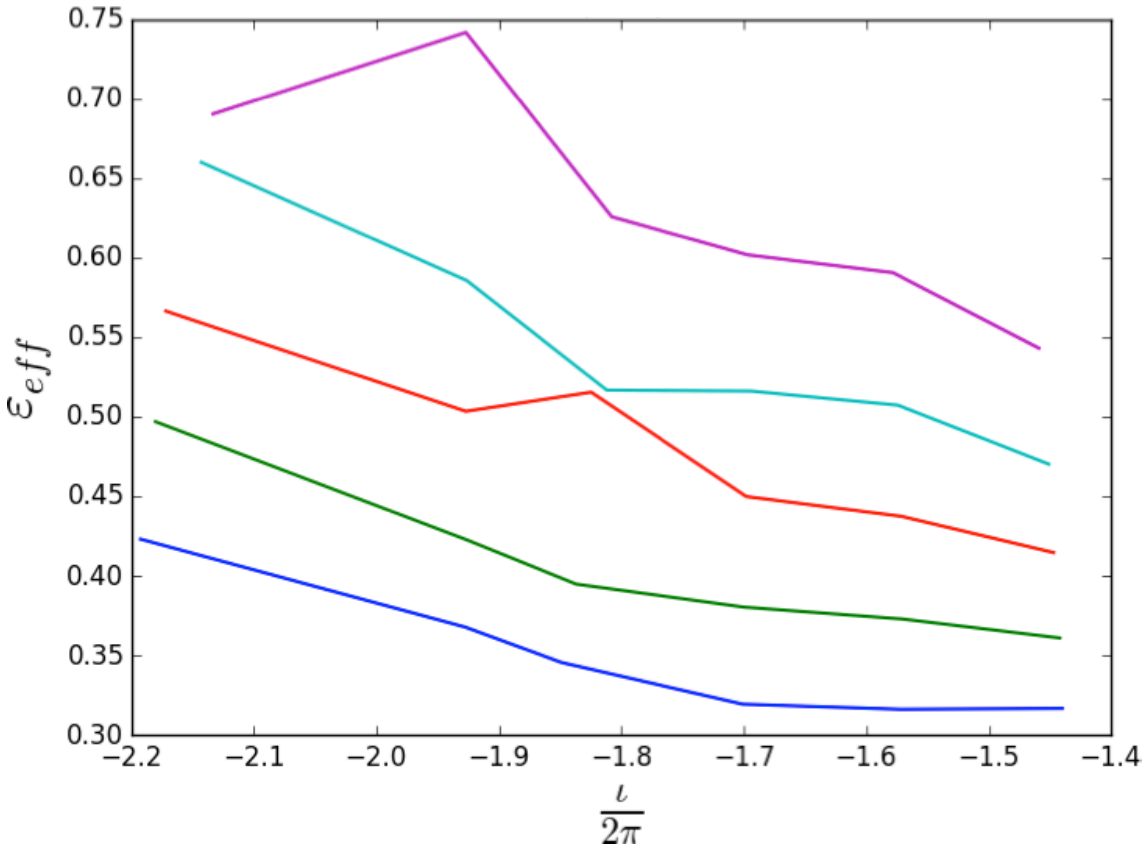
0.75
0.70
0.65
0.60
0.55
0.50
0.45
0.40
0.35
0.30
ε_{eff}
−2.2
−2.1
−2.0
−1.9
−1.8
−1.7
−1.6
−1.5
−1.4
$\frac{\iota}{2\pi}$

Figure 7b.

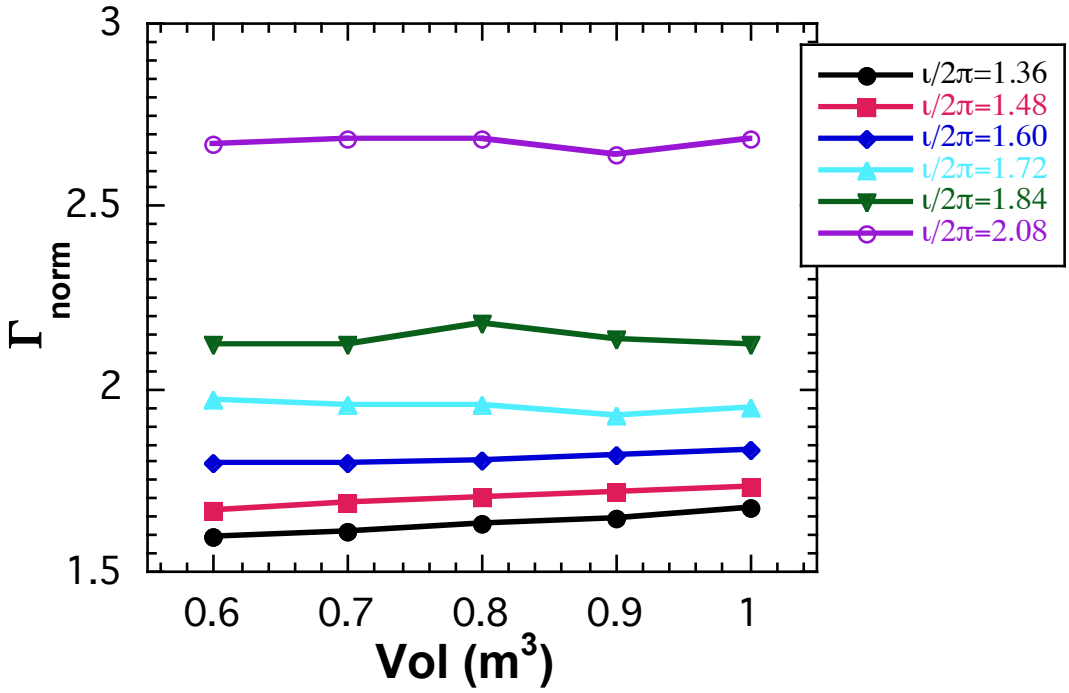
3
2.5
2
1.5
Γ norm
0.6
0.7
0.8
0.9
1
Vol (m3)
ι/2π=1.36
ι/2π=1.48
ι/2π=1.60
ι/2π=1.72
ι/2π=1.84
ι/2π=2.08

Figure 8a.

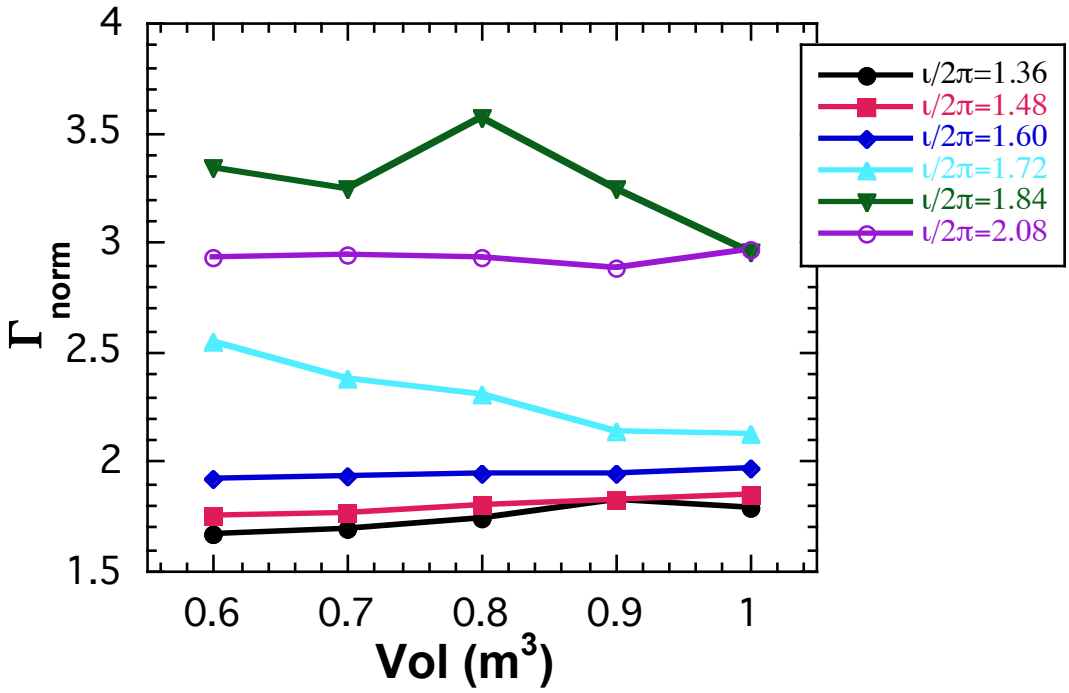
4
3.5
3
2.5
2
1.5
Γ norm
0.6
0.7
0.8
0.9
1
Vol (m3)
ι/2π=1.36
ι/2π=1.48
ι/2π=1.60
ι/2π=1.72
ι/2π=1.84
ι/2π=2.08

Figure 8b.

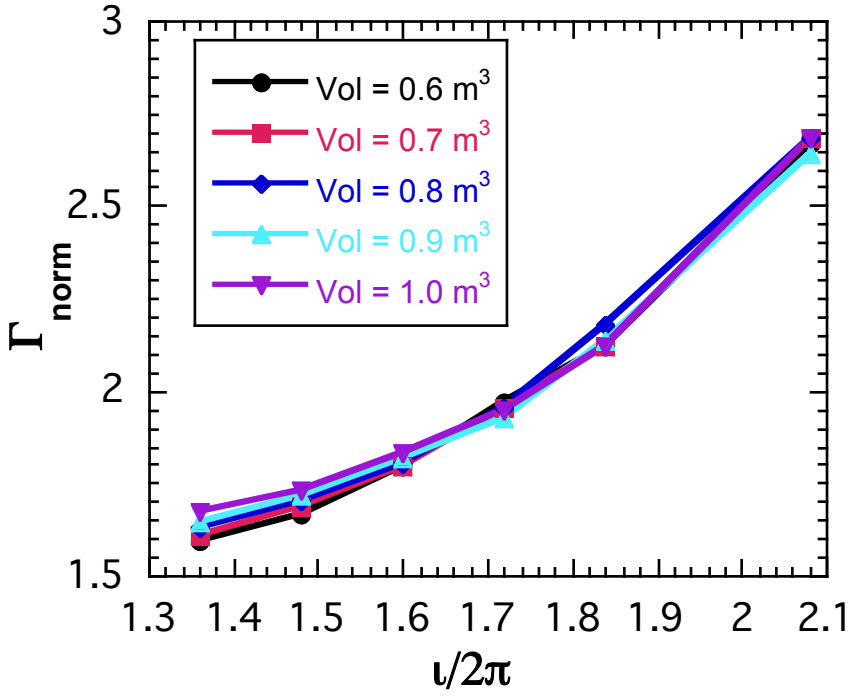
Vol = 0.6 m3
Vol = 0.7 m3
Vol = 0.8 m3
Vol = 0.9 m3
Vol = 1.0 m3
Γ norm
ι/2π
3
2.5
2
1.5
1.3
1.4
1.5
1.6
1.7
1.8
1.9
2
2.1

Figure 9a.

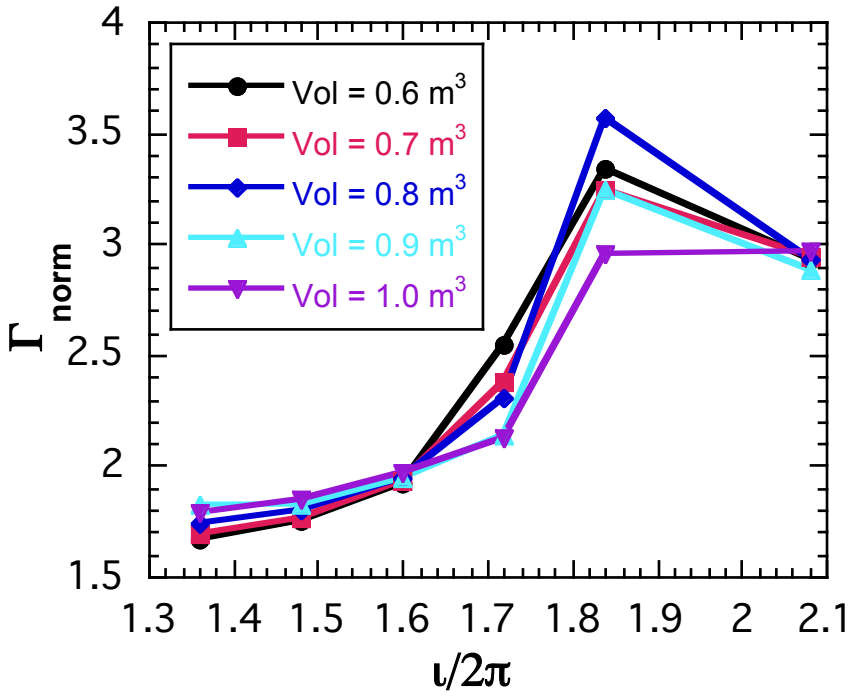
Vol = 0.6 m3
Vol = 0.7 m3
Vol = 0.8 m3
Vol = 0.9 m3
Vol = 1.0 m3
Γ norm
ι/2π
4
3.5
3
2.5
2
1.5
1.3
1.4
1.5
1.6
1.7
1.8
1.9
2
2.1

Figure 9b.

FIGURE CAPTIONS

Figure 1: Coil structure, plasma and vacuum chamber of TJ-II flexible heliac.

Figure 2: Location of the 25 TJ-II configurations used in this work in the flexibility diagram. I_{hc} and I_{cc} are the currents that circulate by the helical and circular coils, respectively, of the central conductor. The lines correspond to constant values of the rotational transform on the axis, indicated in the plot. The dots are located in parallel direction of constant rotational transform while the larger the I_{cc} current, the bigger the volume of the configuration.

Figure 3: Magnetic surfaces of five TJ-II configurations of the scan. The toroidal coil and the vacuum chamber are also represented. Top two configurations correspond to the highest rotational transform, while the bottom ones correspond to the lowest iota values. The right configurations correspond to the larger volumes, while the left ones have smaller volumes. The central one corresponds to intermediate values of volume and iota.

Figure 4: Representation of the effective ripple, as a function of volume and rotational transform in TJ-II. The lines show the different values at different radial positions, where different values of the rotational transform appear.

Figure 5a: Representation of the effective ripple, as a function of volume and rotational transform in TJ-II for ρ=0. The lines extract the dependence of the effective ripple with iota, for constant volume, and with volume, for constant iota.

Figure 5b: Representation of the effective ripple, as a function of rotational transform for five volumes in TJ-II for ρ=0. The five curves correspond to increasing values of the volume from bottom to top.

Figure 6a: The same as figure 5a for ρ=0.65.

Figure 6b: The same as figure 5b for ρ=0.65.

Figure 7a: The same as figures 5a and 6a, for ρ=1.

Figure 7b: The same as figures 5b and 6b, for ρ=1.

Figure 8a: Plateau factor as a function of the volume, for the several values of the rotational transform and for $\rho\approx$0.65.

Figure 8b: Plateau factor as a function of the volume, for the several values of the rotational transform for ρ=1.

Figure 9a: Plateau factor as a function of the rotational transform, for the several values of volume for $\rho\approx$0.65.

Figure 9b: Plateau factor as a function of the rotational transform, for the several values of volume for $\rho\approx$1

References

[1] A. YOSHIZAWA et al. *Plasma Phys. and Control. Fusion* 43 (2001) R1–R144.

[2] H. MAASBERG et al. *Phys. Plasmas* 7(2000) 295.

[3] K. LACKNER AND N.A.O. GOTTARDI. *Nucl. Fusion* 30 (1994) 767

[4] U. STROTH et al. *Nucl. Fusion* 36 (1996) 1063.

[5] H. YAMADA et al. *Nucl. Fusion* 45 (2005) 1684

[6] J. HARRIS. *Plasma Phys. and Control. Fusion* 46 (2004) B77–B90

[7] C. ALEJALDRE et al. *Fusion Sci. and Technology* 17 (1990) 131.

[8] E. ASCASÍBAR, T. ESTRADA, F. CASTEJÓN, A. LÓPEZ-FRAGUAS, I. PASTOR, J. SÁNCHEZ, U. STROTH, J. QIN AND TJ-II TEAM. *Nucl. Fusion* 45 (2005) 276

[9] F. TABARÉS et al. *Plasma Phys. Control. Fusion* 50 (2008) 124051

[10] J. SÁNCHEZ et al. *Nucl. Fusion* 49 (2009) 104018

[11] F. L. HITON AND R. D. HAZELTINE. *Rev. Mod. Phys.* 48 (1976) 239

[12] E. A. BELLI AND J. CANDY. *Plasma Phys. and Control. Fusion* 50 (2008) 095010

[13] S. P. HIRSHMAN, K. C. SHAINGH, W. I. VAN RIJ, C. O. BEASLEY, JR., AND E. C. CRUME, JR. *Phys. Fluids* 29 (1986) 2951

[14] C. BEIDLER et al. *Nucl. Fusion* 51 (2011) 076001

[15] V. V. NEMOV, S. V. KASILOV,W. KERNBICHLER AND M. F. HEYN, *Phys. Plasmas* 6 (1999) 4622

[16] F. CASTEJÓN et al. *Nucl. Fusion* 49 (2009) 085019

[17] S. MURAKAMI, A. WAKASA, H. MAAßBERG, C.D. BEIDLER, H. YAMADA, K.Y. WATANABE AND LHD EXPERIMENTAL GROUP. *Nucl. Fusion* 42 (2002) L19–L22

[18] H. SUGAMA, K. Y. WATANABE, *Phys. Rev. Lett.* 94 (2005) 115001

[19] S. P. GERHARDT, J. N. TALMADGE, J. M. CANIK, AND D. T. ANDERSON *Phys. Rev. Lett.* 94 (2005) 015002

[20] J. L. VELASCO, J. A. ALONSO, I. CALVO, AND J. ARÉVALO. *Phys. Rev. Lett.* 109 (2012) 135003

[21] E. RODRIGUEZ-SOLANO RIBEIRO AND K.C. SHAING, *Phys. Fluids* 30 (1987) 462

[22] A. DINKLAGE, et al, *Nucl. Fusion* 47 (2007) 1265

[23] T. IDO et al. *Nucl. Fusion* 46 (2006) 512

[24] Z. GAO et al. *Phys. Plasmas* 15 (2008) 072511

[25] E. SÁNCHEZ et al. *Plasma Phys and Control. Fusion* 55 (2013) 014015.

[26] F. CASTEJÓN AND A. GÓMEZ-IGLESIAS. "Advances in Grid Computing", Chapter: "Grid Computing for Fusion Research". Ed.: Intech. Rijeka, Croatia, 2011. ISBN 978-953-307-301-9

[27] M. RODRÍGUEZ-PASCUAL, J. GUASP, F. CASTEJÓN, A. J. RUBIO-MONTER, I. M. LLORENTE, R. MAYO. IEEE *Trans. Plasma Sci.* 38 (2010) 2102

[28] M. RODRÍGUEZ-PASCUAL, A. J. RUBIO-MONTERO, R. MAYO, A. BUSTOS, F. CASTEJÓN, et al. Proc of the 18th Euromicro Int. Conf. on Parallel, Distributed and Network-Based Processing (PDP 2011), IEEE CS Press: Ayia Napa, Cyprus, 2011; 380–384.

A. BUSTOS, F. CASTEJÓN, L. FERNÁNDEZ, J. GARCÍA, V. MARTIN-MAYOR, J. REYNOLDS, R. SEKI R, J. L. VELASCO. *Nucl. Fusion* 50 (2010) 125.

[29] F. CASTEJÓN et al. *Plasma Phys and Control. Fusion* 55 (2013) 014003

[30] M. RODRÍGUEZ-PASCUAL, T. SCOTT B, RIBEIRO, F. CASTEJÓN, R. MAYO. *IEEE Transact. Plasma Sci.* 38 (2010) 2111.

[31] A. CAPPA, D. LÓPEZ-BRUNA, F. CASTEJÓN, M. A. OCHANDO, J. L. VÁZQUEZ-POLETTI, et al. *Contr. to Plasma Phys.* 51(2011) 83.

[32] A. J. RUBIO-MONTERO, F. CASTEJÓN, M. A. RODRÍGUEZ-PASCUAL, E. MONTES, R. MAYO. *IEEE Transact. Plasma Sci* 38 (2010) 2093.

[33] J. T. MÓSCICKI, A. BUSTOS, F. CASTEJÓN, J. L. VELASCO, P. MÉNDEZ. "The HEP-Fusion technology transfer using Ganga andDIANE in the EGEE Grid". Proc. of 4th EGEE User Forum 2009. Catania, Italy.

[34] A. GÓMEZ-IGLESIAS, M. A. VEGA-RODRÍGUEZ, F. CASTEJÓN. *App. Soft Comp.* 13 (2013) 2547.

[35] A. J. RUBIO-MONTERO, E. HUEDO, F. CASTEJÓN, R. MAYO-GARCÍA. *Future Generation Computer Systems* 45 (2015) 25.

[36] E. HUEDO, R. S. MONTERO, I. M. LLORENTE. *Future Generation Computer Systems* 23 (2007) 252.